Phase Separation in Jahn-Teller Systems with Localized and Itinerant Electrons

K. I. Kugel, A. L. Rakhmanov, and A. O. Sboychakov
Institute for Theoretical and Applied Electrodynamics, Russian Academy of Sciences, Izhorskaya Street 13/19, Moscow, 125412 Russia

(Received 25 July 2005; published 27 December 2005)

The phase diagram for doped manganites and related compounds is analyzed in terms of the Kondo-lattice model taking into account an interplay between electrons localized due to lattice distortions and those in the band states. It is shown that the number of itinerant charge carriers can be significantly lower than that implied by the doping level. The competition between the homogeneous (ferromagnetic or antiferromagnetic) and phase-separated states is discussed and a strong tendency to the phase separation was revealed for a wide doping range.

DOI: 10.1103/PhysRevLett.95.267210 PACS numbers: 75.47.Lx, 64.75.+g, 71.30.+h, 75.30.−m

Phase separation phenomena play a fundamental role in the physics of strongly correlated electron systems, especially in manganites and related compounds [1–3]. It is commonly believed now that the nature of the colossal magnetoresistance effect is closely related to the phase separation, or to speak more generally, to the formation of inhomogeneous states. The most widely discussed type of phase separation is the formation of nanoscale inhomogeneities such as ferromagnetic (FM) metallic droplets (magnetic polarons or ferrons) located in an insulating antiferromagnetic (AF) matrix. These droplets are formed as a result of a self-trapping of charge carriers. Such a type of phase separation was first predicted by Nagaev for magnetic semiconductors [4]. It is often taken for granted that all charge carriers arising due to doping take part in the formation of FM droplets. However, such an approach can lead to discrepancies with experiment. For example, the size of the droplet turns out to be less than the lattice constant to fit the experimental data on conductivity of $La_{1-x}Mg_xMnO_3$ as was estimated in Ref. [5]. This implies that such a kind of phase separation could exist only for low doping levels, especially in the insulating state. At the same time, the analysis of experimental data demonstrates that the doping level and the number of self-trapped carriers can differ drastically [6]. Therefore, the phase separation manifests itself in a wide region of the phase diagram even at a rather high level of doping [7]. The nature of this difference still remains unclear. Here, we discuss a model relating the doping level and the number of charge carriers.

We consider the picture characteristic of the systems with Jahn-Teller ions with an interplay between electrons localized due to lattice distortions and those in the band states. The situation is typical for manganites and could be described by the Kondo-lattice model in the double exchange limit with an account taken for the Jahn-Teller (JT) distortions. Starting from the seminal Letter [8], such a mechanism was widely discussed in the literature [7,9,10]. Note also Ref. [11], where the localization arises due to AF fluctuations. In Refs. [12,13], this approach was used to analyze the phase diagram of doped manganites. However, the possibility of phase separation was not considered and the difference between the doping level and the density of the itinerant charge carriers was not explicitly addressed. We start with a general two-band Kondo-lattice Hamiltonian, outline the main assumptions to simplify the model, analyze possible homogeneous states, discuss the competition between the homogeneous and phase-separated states, calculate the phase diagram, and briefly discuss the effects of temperature and magnetic field.

Model.—We start from the assumption that in the system with JT ions, an electron can be either localized at the lower level with the energy gain ϵ_{JT} or remain at the higher level decreasing its energy due to band broadening. So, there exists a competition between the localization and the delocalization. We describe the system with localized and band electrons using the Hamiltonian

$$\begin{aligned}
H &= H_{\mathrm{el}} + H_{\mathrm{AF}} + H_{\mathrm{JT}} + H_{\mathrm{el-el}},\\
H_{\mathrm{el}} &= -\sum_{\langle \mathbf{nm}\rangle}\sum_{ab\sigma} t^{ab}_{\mathbf{nm}}(a^{\dagger}_{\mathbf{n}a\sigma}a_{\mathbf{m}b\sigma} + \mathrm{H.c.})\\
&\quad - \frac{J_H}{2}\sum_{\mathbf{n}}\sum_{a\sigma\sigma'} a^{\dagger}_{\mathbf{n}a\sigma}(\vec{\sigma}\mathbf{S}_{\mathbf{n}})_{\sigma\sigma'}a_{\mathbf{n}a\sigma'},\\
H_{\mathrm{AF}} &= J'\sum_{\langle \mathbf{nm}\rangle}\mathbf{S}_{\mathbf{n}}\mathbf{S}_{\mathbf{m}}, \qquad (1)\\
H_{\mathrm{JT}} &= -g\sum_{\mathbf{n}}\sum_{ab\sigma} a^{\dagger}_{\mathbf{n}a\sigma}[Q_{2\mathbf{n}}(\sigma^x)_{ab} + Q_{3\mathbf{n}}(\sigma^z)_{ab}]a_{\mathbf{n}b\sigma}\\
&\quad + \frac{K}{2}\sum_{\mathbf{n}}(Q^2_{2\mathbf{n}} + Q^2_{3\mathbf{n}}),\\
H_{\mathrm{el-el}} &= \frac{U_1}{2}\sum_{\mathbf{n}a\sigma} n_{\mathbf{n}a\sigma}n_{\mathbf{n}a\bar{\sigma}} + \frac{U_2}{2}\sum_{\mathbf{n}a\sigma} n_{\mathbf{n}a\sigma}n_{\mathbf{n}\bar{a}\sigma}.
\end{aligned}$$

Here, $a^{\dagger}_{\mathbf{n}a\sigma}$, $a_{\mathbf{n}a\sigma}$ denote creation and annihilation operators for e_g electrons at site $\mathbf{n}$ with orbital index a ($3z^2 - r^2$ or $x^2 - y^2$) and spin projection σ, $\mathbf{S}_{\mathbf{n}}$ is a local (classical) spin formed by spins of t_{2g} electrons, $\vec{\sigma}$ are the Pauli matrices, and $Q_{2\mathbf{n}}$, $Q_{3\mathbf{n}}$ are normal modes of vibration of MnO_6 octahedron. The terms in H_{el} correspond, respectively, to the kinetic energy of e_g electrons and Hund's rule interaction between e_g electrons and local spins. The second term in H is the Heisenberg AF ($J' > 0$) exchange between local spins. $H_{\rm JT}$ describes the JT interaction between e_g electrons and vibrational modes for MnO$_6$ octahedra, where K is the elastic energy and g is the electron-lattice coupling constant. $H_{\text{el-el}}$ is the on-site Coulomb repulsion between e_g electrons with the same and different orbital indices, where the bar above a or σ means *not a* or *not σ*, respectively.

In the limit $J_H \to \infty$ characteristic of manganites, we can assume that the spin of e_g electrons is parallel to $\mathbf{S_n}$. This implies the transformation of $a_{\mathbf{n}a\sigma}$ to operators $c_{\mathbf{n}a}$ with spin projection $+1/2$ onto the direction of $\mathbf{S_n}$ and also to the transformation of hopping amplitudes: $t^{ab}_{\mathbf{nm}} \to t^{ab}_{\mathbf{nm}}\cos(\nu_{\mathbf{nm}}/2)$, where $\nu_{\mathbf{nm}}$ is the angle between $\mathbf{S_n}$ and $\mathbf{S_m}$ [14]. The JT effect leads to the splitting of the double-degenerate e_g level. As in Ref. [12], we assume that there are two types of e_g electrons in the system: (i) "localized" (l, $t^{(l)}_{\mathbf{nm}} \to 0$) electrons, which produce maximum splitting of the e_g level with the energy gain $-g^2/2K$; (ii) "band" (b) electrons with nonzero hopping integrals $t^{(b)}_{\mathbf{nm}}$ producing smaller distortions of MnO$_6$ octahedra. The effective Hamiltonian then reads

$$\begin{aligned} H'_{\rm eff} &= H_{\rm eff} - \mu\sum_{\mathbf{n}}(n_{l\mathbf{n}} + n_{b\mathbf{n}}), \\ H_{\rm eff} &= -t\sum_{\langle\mathbf{nm}\rangle}(c^\dagger_{\mathbf{n}}c_{\mathbf{m}} + c^\dagger_{\mathbf{m}}c_{\mathbf{n}})\cos\left(\frac{\nu_{\mathbf{nm}}}{2}\right) - \epsilon_{\rm JT}\sum_{\mathbf{n}} n_{l\mathbf{n}} \\ &\quad + J\sum_{\langle\mathbf{nm}\rangle}\cos\nu_{\mathbf{nm}} + U\sum_{\mathbf{n}} n_{l\mathbf{n}}n_{b\mathbf{n}}, \end{aligned} \tag{2}$$

where operators $c^\dagger_{\mathbf{n}}$ and $c_{\mathbf{n}}$ correspond to b electrons and $J = J'S^2$. In Eq. (2), the term with chemical potential μ is added. The summation in the first and the third terms in $H_{\rm eff}$ is performed over nearest neighbors. The effective on-site Coulomb repulsion U in Eq. (2) can differ from U_2, but it has the same order of magnitude (~ 5 eV). $\epsilon_{\rm JT}$ is the JT energy gain for l electrons counting from the center of the b-electron band. Our main assumption is that the effective parameters t and $\epsilon_{\rm JT}$ *do not depend on doping level x*. Preliminary calculations demonstrated that the dependence of t and $\epsilon_{\rm JT}$ on x explicitly taken into account could not significantly affect the obtained results. The number of localized, n_l, and band, n_b, electrons per lattice site obeys an obvious relation $n_b + n_l = 1 - x$.

The suggested model allows us to describe the competition between itinerant and localized electrons as well as the phase separation using a few fitting parameters. So, it can be considered as a minimal model for the physics we wish to outline. Note that Eq. (2) is rather similar to the widely studied Falicov-Kimball model [15], which also exhibits the phase separation [16].

Homogeneous states.—In the homogeneous FM state, $\nu_{\mathbf{nm}} = 0$. The energy spectrum was calculated by the Hubbard I approximation in the equation of motion for b-electron Green functions $G_b(\mathbf{n}, \mathbf{n}_0; t - t_0) = -i\langle Tc_{\mathbf{n}}(t)c^\dagger_{\mathbf{n}_0}(t_0)\rangle$. In the frequency-momentum representation

$$G_b(\mathbf{k}, \omega) = -\frac{\omega + \mu - U(1 - n_l)}{(\omega + \mu - E_1(\mathbf{k}))(\omega + \mu - E_2(\mathbf{k}))}, \tag{3}$$

where

$$E_{1,2}(\mathbf{k}) = \frac{U + \varepsilon(\mathbf{k})}{2} \mp \sqrt{\left(\frac{U - \varepsilon(\mathbf{k})}{2}\right)^2 + U\varepsilon(\mathbf{k})n_l}, \tag{4}$$

and $\varepsilon(\mathbf{k})$ is the energy spectrum at $U = 0$. For a simple cubic lattice $\varepsilon(\mathbf{k}) = -2t(\cos k_x + \cos k_y + \cos k_z)$. If $n_b \leq 0.5$, at any realistic temperature the upper subband (4) is empty for any doping level.

The numbers of localized and band electrons depend on the relative positions of μ and $\epsilon_{\rm JT}$. If $\mu < -\epsilon_{\rm JT}$, then $n_l = 0$ and $n_b = 1 - x$. With the increase of n_b, μ becomes equal to $-\epsilon_{\rm JT}$, the further growth in the number of itinerant charge carriers is unfavorable, n_l is nonzero, and μ is pinned at the level $-\epsilon_{\rm JT}$. Using the relation for the density of states $\rho_0(E) = -\pi^{-1}{\rm Im}\int G_b(\mathbf{k}, E + i0)d^3\mathbf{k}/(2\pi)^3$, we obtain in the limit $U \gg w_0 = zt$

$$\begin{aligned} n_b &= \int_{-w_0(1-n_l)}^{-\epsilon_{\rm JT}} dE\rho_0(E) \\ &= (1 - n_l)\int_0^{+\infty}\frac{d\tau}{\pi}\,\frac{\sin(w_0\tau) - \sin(\tau\frac{\epsilon_{\rm JT}}{1-n_l})}{\tau}J_0^3\left(\frac{2w_0\tau}{z}\right), \end{aligned} \tag{5}$$

where $z = 6$ is the number of nearest neighbors in the cubic lattice and J_0 is the Bessel function. The last integral corresponds to $\varepsilon(\mathbf{k})$ for the simple cubic lattice. Equation (5) and condition $n_b + n_l = 1 - x$ define n_b as a function of x. In our model, there are two critical values of x, x_1 and x_2. If $x < x_1 = \epsilon_{\rm JT}/w_0$, then $n_b = 0$, as it readily follows from Eq. (5). In this case, the homogeneous FM state does not exist. At $x = x_2$ the number of localized electrons vanishes. The value of x_2 can be found from Eq. (5) at $n_l = 0$. The dependence of n_l and n_b on x is shown in Fig. 1 for typical parameters of the model. Note that n_b does not exceed 0.5 as was assumed above.

At $x_1 < x < x_2$, the energy per site is equal to $E_{\rm FM} = E_{\rm kin} - \epsilon_{\rm JT}n_l + zJ$, where

$$E_{\rm kin} = \int_{-w_0(1-n_l)}^{-\epsilon_{\rm JT}} dEE\rho_0(E) \tag{6}$$

is the kinetic energy of b electrons. At $x > x_2$, we have $n_l = 0$, and $-\epsilon_{\rm JT}$ in Eqs. (5) and (6) is substituted by the chemical potential μ. Thus, $E_{\rm FM} = E_{\rm kin}(\mu) + zJ$, with μ determined from Eq. (5). Function $E_{\rm FM}(x)$ is shown in Fig. 2. For a spherical Fermi surface (small band filling,

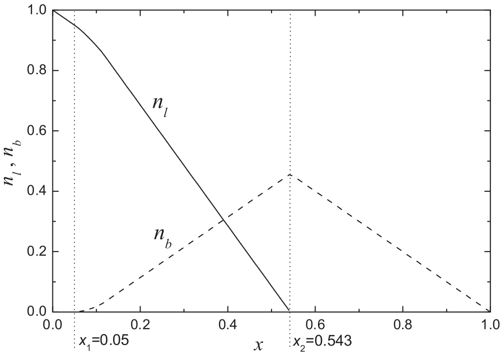

FIG. 1. n_l (solid line) and n_b (dashed line) vs doping level x; $\epsilon_{\mathrm{JT}}/w_0 = 0.05$; $j = zJ/w_0 = 0.005$.

$n_b \ll 1$), E_{kin} can be written as

$$E_{\mathrm{kin}} \simeq -(1-n_l)w_0 n_b\left[1 - \frac{3}{5z}\left(\frac{6\pi^2 n_b}{1-n_l}\right)^{2/3}\right]. \quad (7)$$

In the homogeneous AF state, we have $\nu_{\mathbf{nm}} = \pi$. At high values of J_H, the formation of itinerant electrons is suppressed and the energy of the AF phase is $E_{\mathrm{AF}} = -\epsilon_{\mathrm{JT}}(1-x) - zJ$; see the dashed line in Fig. 2. We can see that the AF state is favorable in energy both at small values of x and near $x = 1$. Note that these results are obtained without taking into account the charge ordering, which could be an additional source of localization at $x \gtrsim 0.5$.

The uniform canted state could be studied by the same method as FM and AF states accounting that $0 < \nu_{\mathbf{nm}} < \pi$. However, the analysis shows that in the parameter range characteristic of manganites ($U > J_H \gg t \gg J$), the uniform canted state is unfavorable. It is more so if we take into consideration a possibility of the phase separation, which we discuss below.

Phase separation.—Here we discuss the possible separation of the system into FM regions containing itinerant electrons and AF regions with $n_b = 0$. The energies of FM and AF homogeneous states have minima at $x = x_2$ and $x = 0$, respectively; see Fig. 2. This indicates that the effective doping level in the FM state, x_f, and in the AF state, x_a, could be different obeying the condition $px_f + (1-p)x_a = x$, where p is the FM phase content. In the calculation of the energy of the phase-separated (PS) state, we should take into account the Coulomb term due to the redistribution of the charge density and the finite size of inhomogeneities. A due account of this contribution allows one to find a characteristic size of the inhomogeneities [17]. Both additional terms depend on the structure of the inhomogeneous state. Here, we use the simplest geometry of the PS regions; i.e., at $p < 0.5$, we have the spheres of the FM phase embedded into the AF matrix, and at $p > 0.5$ AF spheres are within the FM matrix.

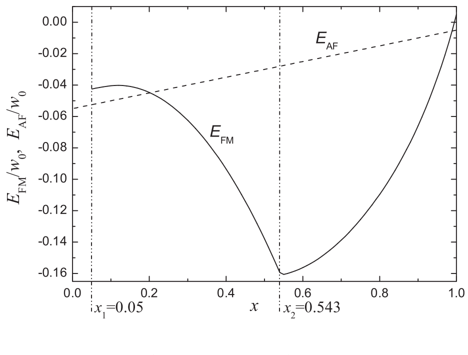

FIG. 2. The energy of the system in FM (solid line) and AF (dashed line) states vs doping level x; $\epsilon_{\mathrm{JT}}/w_0 = 0.05$; $j = zJ/w_0 = 0.005$.

To calculate the Coulomb energy, we divide the system into spherical cells of radius R_c. In the center of the cell we have the FM or AF sphere of radius R_s, which is defined by the electroneutrality condition: $R_s = p^{1/3}R_c$ for $p < 0.5$ and $R_s = (1-p)^{1/3}R_c$ for $p > 0.5$. Following Ref. [17], we can write the Coulomb energy per site E_c at $p < 0.5$ as

$$E_c = \frac{2\pi e^2}{5\epsilon d}(x_f - x_a)^2\left(\frac{R_s}{d}\right)^2 p(2 - 3p^{1/3} + p), \quad (8)$$

where ϵ is the permittivity and d is the lattice constant. For $p > 0.5$, we should replace $x_f \leftrightarrow x_a$ and $p \rightarrow 1 - p$.

Since in the PS state b electrons are confined within a finite region, we should take into account the corrections to the electron density of states due to the dimensional quantization. At $p < 0.5$, it is convenient to express the corresponding contribution to the energy in the form

$$E_s = p\frac{3d}{R_s}\sigma(x_f). \quad (9)$$

For $p > 0.5$, we should replace p by $1 - p$. Note that $\sigma(x_f)$ does not depend explicitly on x_a since there are no itinerant electrons in the AF phase. The value of $\sigma(x_f)$ was calculated for small d/R_s ratios following the approach of Refs. [18,19] for the simple cubic lattice. Within the order of magnitude, $\sigma(x_f)$ can be estimated as $tn_b^{4/3}(x_f)$.

Terms (8) and (9) determine an optimum size of inhomogeneities. Minimizing $E_{cs} = E_c + E_s$ with respect to R_s, at $p < 0.5$ one obtains

$$R_s = d\left[\frac{15\sigma(x_f)}{4\pi u(x_f - x_a)^2(2 - 3p^{1/3} + p)}\right]^{1/3}, \quad (10)$$

$$E_{cs} = 3p\left[\frac{9\pi u}{10}(x_f - x_a)^2\sigma^2(x_f)(2 - 3p^{1/3} + p)\right]^{1/3}, \quad (11)$$

where $u = e^2/\epsilon d$. At $p > 0.5$, we should replace p by $1 - p$ and use the corresponding value of $\sigma(x_f)$. Our calculations are applicable if the inhomogeneity contains a relatively large number of lattice sites. For characteristic values of parameters we find $R_s/d = 1.5 - 3$.

To find concentrations of each phase, it is necessary to minimize the total energy $E_{\mathrm{PS}} = pE_{\mathrm{FM}}(x_f) + (1-p)E_{\mathrm{AF}}(x_a) + E_{cs}(x_f, x_a, p)$ with respect to x_f and x_a. To find the range of doping where the PS is favorable, we

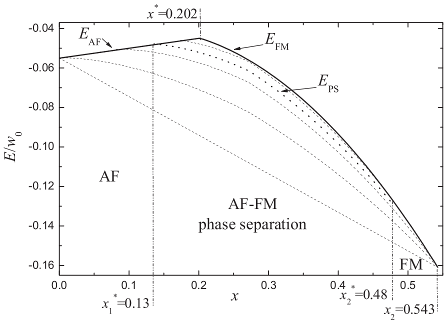

FIG. 3. The energy of the system vs doping level x. The solid line corresponds to the homogeneous (AF at $x < x^*$ or FM at $x > x^*$) state. The dashed lines correspond to energies of the phase-separated state calculated at $u/w_0 = 2, 3/2, 1, 1/4, 0$ from up to down. Other parameters are $\epsilon_{\mathrm{JT}}/w_0 = 0.05$ and $j = zJ/w_0 = 0.005$. The regions of stability of AF, FM, and AF-FM phase-separated states are shown at $u/w_0 = 3/2$.

compare E_{PS} with energies of homogeneous states. In Fig. 3, we plot E_{PS} vs x at different values of u. The energies of the homogeneous states are also shown. This figure demonstrates that in the limit $u \to 0$ the PS state is favorable within the $0 < x < x_2$ doping range. When u is increased, the range of phase separation gradually narrows and disappears at $x = x^*$, where $E_{\mathrm{FM}} = E_{\mathrm{AF}}$. A homogeneous state can correspond to a local energy minimum, but in our model, it can appear only due to the intersite Coulomb interaction related to the charge redistribution. If this interaction is weak, a homogeneous state becomes absolutely unstable. The situation is similar to the phase separation in the usual Kondo-lattice model where the compressibility of a homogeneous state is negative [3].

Conclusions.—A "minimal model" dealing with the competition between the localization and metallicity in manganites was formulated. We demonstrated that the number of itinerant charge carriers can be significantly lower than that implied by the doping level. A strong tendency to the phase separation was revealed for a wide range of intermediate doping concentrations vanishing at low and high doping levels. These predictions are in agreement with the experimentally found phase diagram of manganites [2,7]. The latter result, alongside with the calculated size of ferron, could serve as a key to an adequate description of the transport properties of manganites that could not be done in the framework of the single-band models [6]. As it was mentioned above, Hamiltonian (2) is analogous in several aspects to the Falicov-Kimball model used in the analysis of heavy-fermion materials. So, we believe that our approach could be applicable not only to manganites but also to a wider class of strongly correlated electron systems.

Our minimal model does not take into account the possibility of charge ordering, which could change the results for x near 0.5. Note that the canted state was predicted in Ref. [13] for charge-ordered phases, but the possibility of phase separation was not considered there. The results were obtained at zero applied magnetic field H and temperature T, but our approach can be directly generalized to finite H and T. It is evident that an increase in H favors the FM state. The effect of temperature manifests itself mainly in the change of the effective hopping integral t due to the polaron band narrowing [20,21] and the entropy term in the free energy due to thermal fluctuations of local spins. When the entropy term dominates over the polaron band narrowing, FM regions can exist in the paramagnetic surrounding and this situation can be also described within the model.

The work was supported by the Russian Foundation for Basic Research Grant No. 05-02-17600 and by the Russian Presidential Grant No. NSh-1694.2003.2.

[1] E. L. Nagaev, Phys. Rep. **346**, 387 (2001).

[2] E. Dagotto, T. Hotta, and A. Moreo, Phys. Rep. **344**, 1 (2001).

[3] M. Yu. Kagan and K. I. Kugel, Usp. Fiz. Nauk **171**, 577 (2001); [Phys. Usp. **44**, 553 (2001)].

[4] E. L. Nagaev, Pis'ma Zh. Eksp. Teor. Fiz. **6**, 484 (1967); [JETP Lett. **6**, 18 (1967)].

[5] J. H. Zhao, H. P. Kunkel, X. Z. Zhou, and G. Williams, Phys. Rev. B **66**, 184428 (2002).

[6] K. I. Kugel, A. L. Rakhmanov, A. O. Sboychakov, M. Yu. Kagan, I. V. Brodsky, and A. V. Klaptsov, Zh. Eksp. Teor. Fiz. **125**, 648 (2004); [JETP **98**, 572 (2004)].

[7] E. Dagotto, *Nanoscale Phase Separation and Colossal Magnetoresistance* (Springer-Verlag, Berlin, 2003).

[8] A. J. Millis, P. B. Littlewood, and B. I. Shraiman, Phys. Rev. Lett. **74**, 5144 (1995).

[9] J. Bala, P. Horsch, and F. Mack, Phys. Rev. B **69**, 094415 (2004).

[10] M. Gulacsi, A. Bussmann-Holder, and A. R. Bishop, Phys. Rev. B **71**, 214415 (2005).

[11] J. J. Betouras and S. Fujimoto, Phys. Rev. B **59**, 529 (1999).

[12] T. V. Ramakrishnan, H. R. Krishnamurthy, S. R. Hassan, and G. V. Pai, Phys. Rev. Lett. **92**, 157203 (2004).

[13] O. Cépas, H. R. Krishnamurthy, and T. V. Ramakrishnan, Phys. Rev. Lett. **94**, 247207 (2005).

[14] P. G. de Gennes, Phys. Rev. **118**, 141 (1960).

[15] L. M. Falicov and J. C. Kimball, Phys. Rev. Lett. **22**, 997 (1969).

[16] J. K. Freericks, Ch. Gruber, and N. Macris, Phys. Rev. B **60**, 1617 (1999); J. K. Freericks, E. H. Lieb, and D. Ueltschi, Phys. Rev. Lett. **88**, 106401 (2002); M. M. Maśka and K. Czajka, Phys. Status Solidi (b) **242**, 479 (2005).

[17] J. Lorenzana, C. Castellani, and C. di Castro, Europhys. Lett. **57**, 704 (2002).

[18] R. Balian and C. Bloch, Ann. Phys. (N.Y.) **60**, 401 (1970).

[19] I. González, J. Castro, and D. Baldomir, Phys. Lett. A **298**, 185 (2002).

[20] A. S. Alexandrov and N. F. Mott, *Polarons and Bipolarons* (World Scientific, Singapore, 1995).

[21] K. I. Kugel and D. I. Khomskii, Zh. Eksp. Teor. Fiz. **79**, 987 (1980); [Sov. Phys. JETP **52**, 501 (1980)].